catalysts

MDPI

Article

Enhancement on $PrBa_{0.5}Sr_{0.5}Co_{1.5}Fe_{0.5}O_5$ Electrocatalyst Performance in the Application of Zn-Air Battery

Chengcheng Wang [1,†], Ziheng Zheng [1,†], Zian Chen [1], Xinlei Luo [1], Bingxue Hou [2], Mortaza Gholizadeh [3], Xiang Gao [1], Xincan Fan [1,*] and Zanxiong Tan [1,*]

[1] School of Entrepreneurship and Innovation, Shen Zhen Polytechnic, Shenzhen 518055, China; wangchengcheng@szpt.edu.cn (C.W.); zzh13410459434@hotmail.com (Z.Z.); cza321654@hotmail.com (Z.C.); lznra@outlook.com (X.L.); gaoxiang@szpt.edu.cn (X.G.)
[2] Aviation Engineering Institute, Civil Aviation Flight University of China, Guanghan 618037, China; bingxuehou@foxmail.com
[3] Faculty of Chemical and Petroleum Engineering, University of Tabriz, Tabriz 51666, Iran; morteza_gh2000@yahoo.com
* Correspondence: horsefxc@szpt.edu.cn (X.F.); tanzanxiong@szpt.edu.cn (Z.T.)
† These authors contributed equally to this work.

Abstract: Due to the insufficient stability and expensive price of commercial precious metal catalysts like Pt/C and IrO_2, it is critical to study efficiently, stable oxygen reduction reaction as well as oxygen evolution reaction (ORR/OER) electrocatalysts of rechargeable Zn-air batteries. $PrBa_{0.5}Sr_{0.5}Co_{1.5}Fe_{0.5}O_5$ (PBSCF) double perovskite was adopted due to its flexible electronic structure as well as higher electro catalytic activity. In this study, PBSCF was prepared by the citrate-EDTA method and the optimized amount of PBSCF-Pt/C composite was used as a potential ORR/OER bifunctional electrocatalyst in 0.1 M KOH. The optimized composite exhibited excellent OER intrinsic activity with an onset potential of 1.6 V and Tafel slope of 76 mV/dec under O_2-saturated 0.1 M KOH. It also exhibited relatively competitive ORR activity with an onset potential of 0.9 V and half-wave potential of 0.78 V. Additionally, Zn–air battery with PBSCF composite catalyst showed relatively good stability. All these results illustrate that PBSCF-Pt/C composite is a promising bifunctional electrocatalyst for rechargeable Zn-air batteries.

Keywords: $PrBa_{0.5}Sr_{0.5}Co_{1.5}Fe_{0.5}O_5$; double perovskite; ORR; OER; rechargeable Zn-air battery

check for updates

Citation: Wang, C.; Zheng, Z.; Chen, Z.; Luo, X.; Hou, B.; Gholizadeh, M.; Gao, X.; Fan, X.; Tan, Z. Enhancement on $PrBa_{0.5}Sr_{0.5}Co_{1.5}Fe_{0.5}O_5$ Electrocatalyst Performance in the Application of Zn-Air Battery. *Catalysts* **2022**, *12*, 800. https://doi.org/10.3390/catal12070800

Academic Editors: Vladimir Guterman, Sergey Belenov and Anastasia Alekseenko

Received: 23 June 2022
Accepted: 13 July 2022
Published: 20 July 2022

1. Introduction

Nowadays, the increasing demand for safe, clean and renewable energy in society has inspired scientists to conduct extensive research on electrochemical energy storage and conversion technologies. Due to their rich resources, high specific energy density and the fact that it is environmentally benign, metal-air batteries have become the main research hotspots. Zn-air battery [1–4] is considered an efficient metal-air battery with a cheap price, good energy density and safety. However, its wide application is greatly restricted by the slow kinetics of ORR [5] and OER [6] due to complicated reduction, oxidation processes including breaking OH bonds and forming O=O bonds. Therefore, this greatly affects the efficiency and practicability of these electrochemical energy devices. Precious metal catalysts such as Pt/C, IrO_2 etc. are widely adopted to achieve superior ORR and OER performance [6], but their high price and scarcity limit significantly their wide application in the energy devices. Moreover, they are quite unstable when being used in alkaline condition. Hence, it is urgent to develop a cheap, high-performing and stable electrocatalyst. Much more attention has been paid to prepare non-precious-metal ORR and OER electrocatalysts by using transition metal oxides and carbon-based electrocatalysts [7–9]. Transition metal oxides composites exhibiting high bifunctional ORR and OER activities have been extensively studied due to their easily tailoring surface properties as well as sufficient catalytic activity.

Among transition metal oxides composites, perovskites are one of the most suitable electrocatalysts due to their easy preparation method as well as tunable structure by adjusting A site or B site cations in the ABO_3 compound [10–13]. Firstly, Suntivich et al. [14,15] prepared excellent OER perovskite electrocatalysts because of e_g orbital of the transition metal. $Ba_{0.5}Sr_{0.5}Co_{0.8}Fe_{0.2}O_{3-\delta}$ (BSCF) [14] exhibits higher OER compared to IrO_2. However, BSCF is not stable after long-time operation due to the amorphous structure. There are many studies regarding the optimization of ORR and OER performances of perovskites by different site doping [16–23]. Our group [24] ever reported that $La_{0.5}Sr_{0.5}Ni_{0.4}Fe_{0.6}O_{3-\delta}$ was a promising catalyst with high OER activity under alkaline condition; however, the long-term stability of the perovskite electrocatalysts was not extensively studied yet. $SrCo_{0.95}P_{0.05}O_{3-\delta}$ (SCP) [18] perovskite electrocatalysts were studied by Yilong Zhu et al., who found that OER activity as well as the stability can be enhanced by doping with a certain amount of P element into B site. Recently, their group continuously investigated $Sr(Co_{0.8}Fe_{0.2})_{0.95}P_{0.05}O_{3-\delta}$ bifunctional electrocatalysts in Zn-air batteries. Their studies indicated that the optimized amount of $Sr(Co_{0.8}Fe_{0.2})_{0.95}P_{0.05}O_{3-\delta}$-Pt composite can exhibit excellent ORR/OER activity [25]. In addition, they showed that the initial discharge potential was 1.25 V, while the charge potential was 2.02 V with excellent stability at 5 mA/cm^2. Therefore, there are many ways to develop perovskite catalysts with better activity in the field of Zn-air batteries.

More attention is given to double perovskites due to the flexible electronic structure, defect introduction, surface modification, nanostructures as well as higher activity. Moreover, they were much cheaper than commercial precious metal electrocatalysts. $NdBa_{0.5}Sr_{0.5}Co_{1.5}Fe_{0.5}O_5$ catalysts exhibited better activity and stability than single perovskite electrocatalysts [26]. Shao Z.P. et al. [27] also reported that $Ba_2CoMo_{0.5}Nb_{0.5}O_6$ was an active OER catalyst under alkaline conditions and it had excellent stability in an alkaline medium. In this study, $PrBa_{0.5}Sr_{0.5}Co_{1.5}Fe_{0.5}O_5$ electrocatalysts were synthesized by the traditional EDTA-citrate method and evaluated as potential bifunctional ORR/OER electrode materials for aqueous rechargeable Zn-air battery under alkaline condition. It was also used in the solid Zn-air battery [28–32]. Additionally, the structure and electrochemical performance of $PrBa_{0.5}Sr_{0.5}Co_{1.5}Fe_{0.5}O_5$ electrode were studied. This work not only represents the advancement direction in highly efficient bifunctional electrocatalysts, but also widens the application of these electrocatalysts in rechargeable metal-air batteries, especially solid Zn air batteries.

2. Results and Discussion

2.1. Phase as well as Microstructure Identification

Figure 1a shows the XRD pattern of PBSCF combusted at 1000 °C for 5 h with the double pervoskite phase, which was in accordance with other researchers' reported results [16]. The main perovskite phase was similar to JCPDS card 46-0335. The minor peaks that appeared at 26°, 36° and 43° might referred to $Sr_2Fe_2O_5$, which might need more investigations. According to the SEM image, PBSCF particles were mostly dispersing uniformly with a particle size of 100–200 nm, which was similar to TEM results as shown in Figure 1c. Interestingly, it is worth mentioning that there were some tiny particles observed in Figure 1b as well. EDX results showed that these particles were still mainly composed of PBSCF elements, and the peak intensity of Sr and Fe was more obvious, which might indicate that Sr-related compounds formed. This was similar to XRD results of minor peaks. The d-spacing of 0.297 nm was indexed to the (110) plane of perovskites The selected-area electron diffraction (SAED) pattern of nanoparticles was shown in Figure 1d, which demonstrated that PBSCF showed Debye Scherer rings, which confirms that it has a crystalline structure.

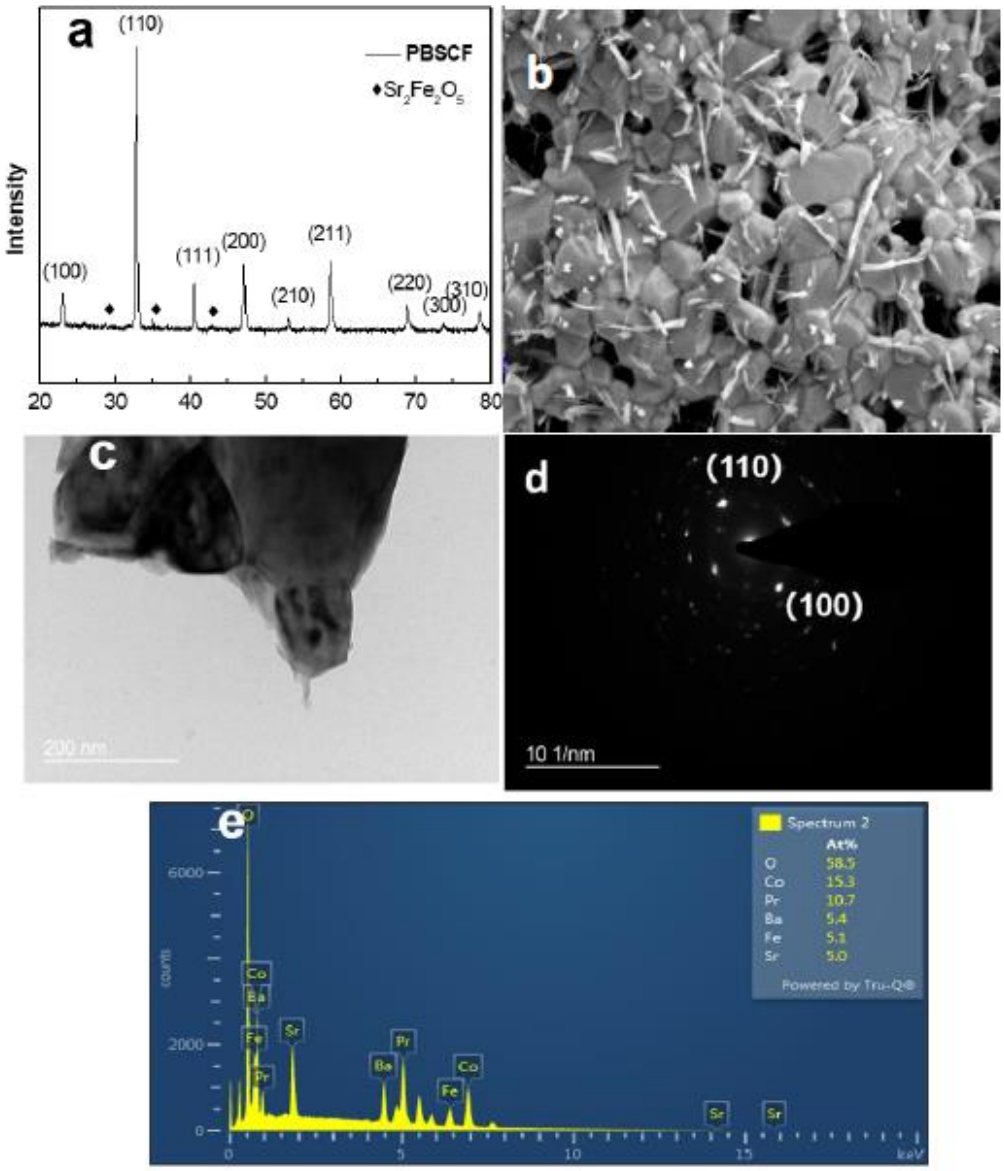

Figure 1. XRD for $PrBa_{0.5}Sr_{0.5}Co_{1.5}Fe_{0.5}O_5$ (PBSCF) (**a**) powders prepared by EDTA-citrate method fired at 1000 °C for 5 h. SEM images of as-prepared PBSCF (**b**). TEM images of the as-prepared PBSCF (**c**) the diffraction pattern as shown in (**d**), and the EDS of selected point was shown in (**e**).

The oxidation states of PBSCF were evaluated by XPS to investigate the origin of the electrocatalytic activity. Figure 2a shows the survey scan of the catalysts for PBSCF electrocatalysts, indicating the presence of Ba, Sr, Co, Fe and O elements. Some unknown peaks might be due to contamination during the tests like Na, Cl and so on. Deconvoluted O 1s spectra is shown in Figure 2b. The peaks were divided into four individual species like surface adsorbed water species OH^-, O^-, and O^{2-}. The relative amount of O^- was related to the concentration of surface oxygen species contributing to superior oxygen reduction electrcatalytic activity [25].

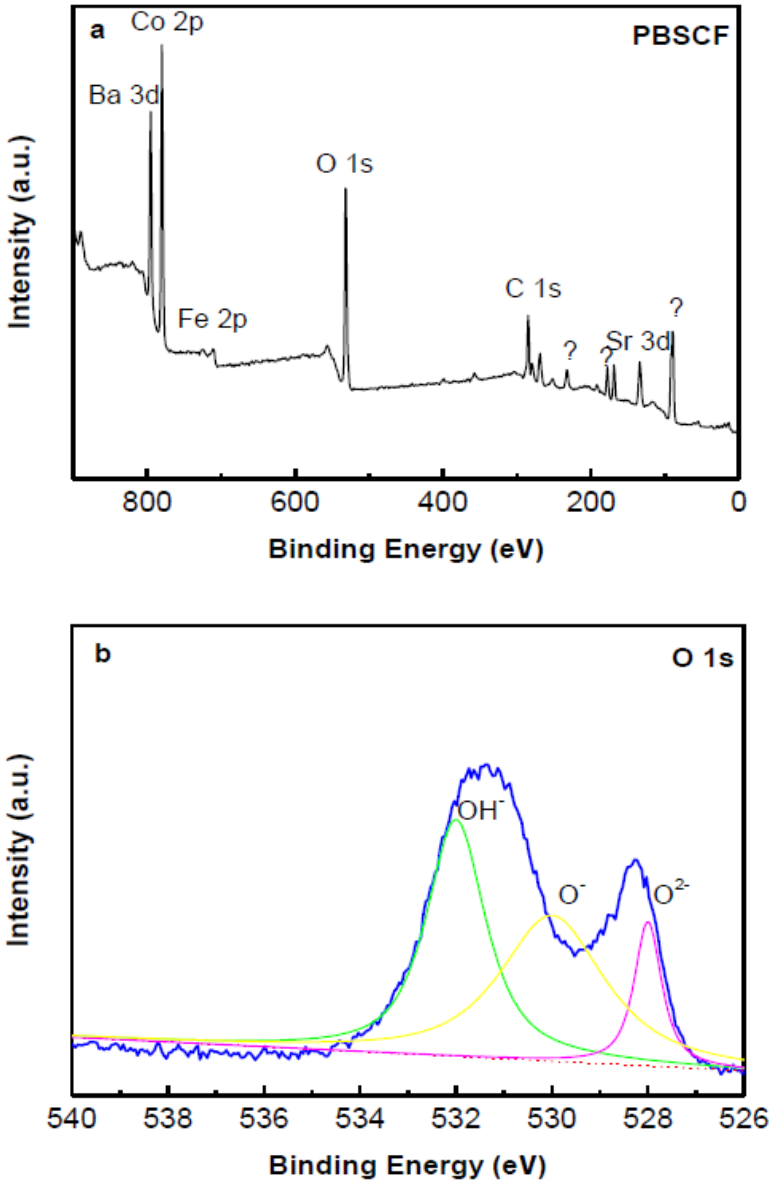

Figure 2. Survey Scan of PBSCF of XPS spectra (**a**), High resolution deconvoluted of O 1s spectra of PBSCF electrocatalysts (**b**).

2.2. Electrocatalytic Activity

Figure 3a,b shows ORR activity of Pt/C from 400 to 2500 rpm, PBSCF, and PBSCF composite electrodes under O_2-saturated 0.1 M KOH at 10 mV/s at 1600 rpm. The onset potential and half wave potential of the PBSCF electrode were 0.7 V, and 0.5 V, respectively. While onset potential as well as half wave potential of PBSCF composite were 0.9 V and 0.78 V, respectively. Obvious synergistic effect of PBSCF and Pt/C might be accounted for this phenomenon. The outstanding electrochemical activities observed might be explained by analysing the O peak of the XPS result, and the relative amount of these oxidative oxygen species (O^{2-}/O^{-}) was closely correlated with the concentration of surface oxygen species, which contributed to good ORR and OER activities. For commercial Pt/C, onset potential and half wave potential was 0.9 V, 0.8 V, respectively. OER activity of Pt/C, PBSCF, and PBSCF composite electrodes was also evaluated at the same condition (Figure 3c). Onset potential of PBSCF composite was 1.58 V, which was 60 mV higher than IrO_2 (1.52 V). Maximum current density measured at 1.9 V was 12 mA/cm^2, which was higher than IrO_2 (9 mA/cm^2). Moreover, the onset potential of PBSCF was around 1.62 V. Remarkably, PBSCF composite afforded current density (10 mA/cm^2) at 1.81 V.

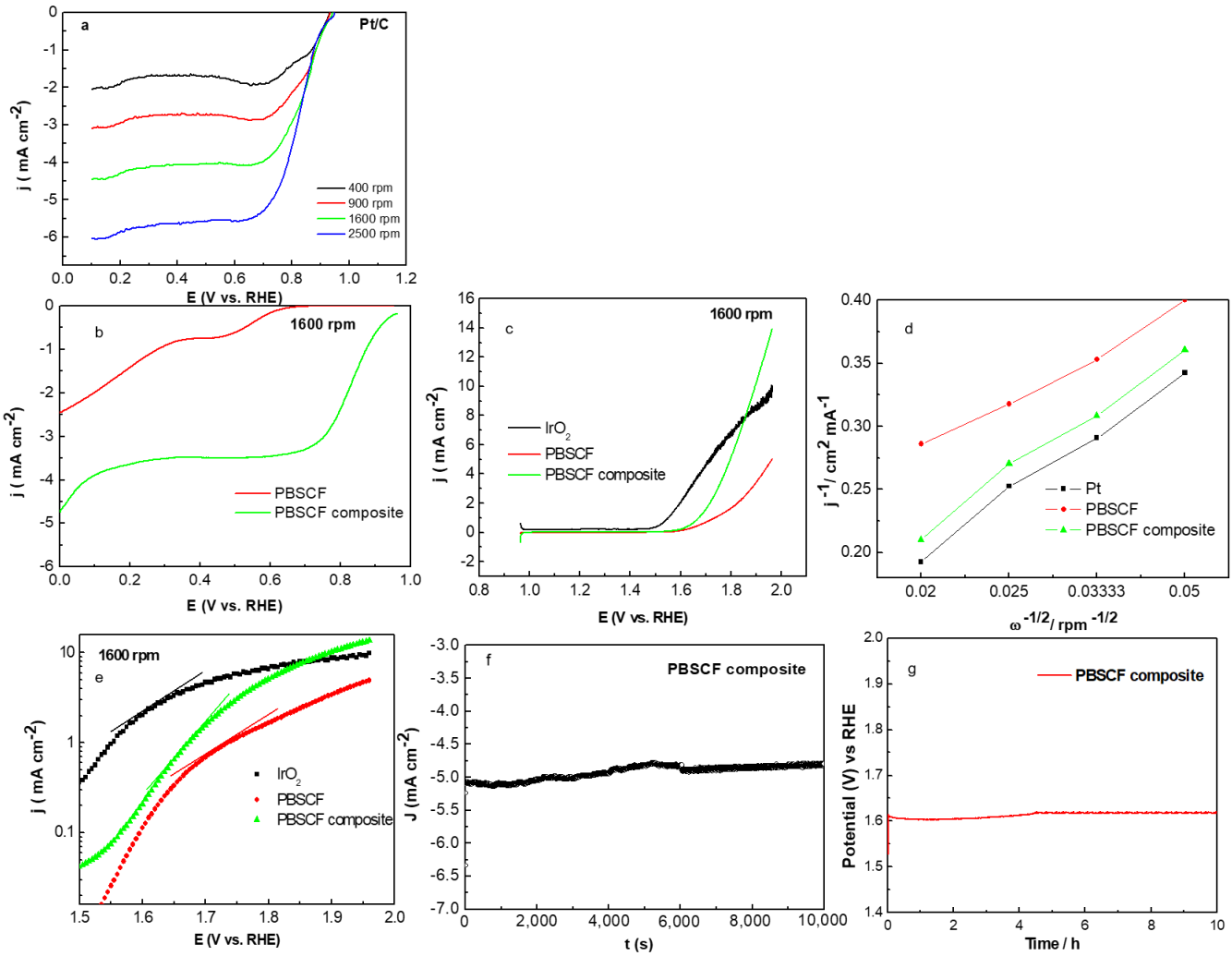

Figure 3. ORR activity of LSV curves for (**a**) 20 Pt/C, (**b**) PBSCF, and PBSCF composite, (**c**) OER activity of LSV curves for PBSCF, 20 Pt/C, and PBSCF composite, (**d**) K-L plots for PBSCF, 20 Pt/C, and PBSCF composite, (**e**) Tafel plots for PBSCF, 20 Pt/C, and PBSCF composite, (**f**) Chronopotentiometry curves of ORR for PBSCF composite at 0.41 V. (**g**) Chronoamperometry curves of OER for PBSCF composite at 10 mA cm^{-2} tested at 1600 rpm in O_2-saturated 0.1 M KOH solution.

Figure 3d shows ORR kinetics evaluated by Koutecky-Levich (K-L) equation. Electron transfer numbers for Pt/C and PBSCF composite were nearly 4.0. $4e^-$ reduction was predominant for PBSCF composite. Figure 3e shows Tafel slope plots of PBSCF, IrO_2 and PBSCF composite measured under O_2 saturated 0.1 M KOH at 0.1 mV/s. Tafel slope for PBSCF composite was 76 mV/dec, while PBSCF was 89 mV/dec. Zhu. reported that Tafel slope for $SrNb_{0.1}Co_{0.7}Fe_{0.2}O_3$ and BSCF were 76 and 94 mV/dec, respectively [16]. The Tafel slope of IrO_2 was 60mV/dec. The relatively lower Tafel slopes for PBSCF composite might indicate the synergistic effect for Pt and PBSCF.

Chronopotentiometry ORR stability for PBSCF composite was also studied at a constant potential of 0.75 V (Figure 3f) with the same loading condition. PBSCF composite showed good ORR stability. It initially reached 4.9 mA/cm^2 and then became 5.2 mA/cm^2 after 10,000 s. Chronoamperometry OER stability for PBSCF composite was obtained at 10 mA/cm^2 (Figure 3f). The initial potential for PBSCF composite was 1.6 V, and it was approximately 1.62 V after 10 h.

2.3. Cell Performance

PBSCF composite electrocatalyst assembled in an aqueous rechargeable Zn-air battery was tested. Three Zn-air batteries could power the LED screen continuously (Figure 4). OCVs of PBSCF composite-based Zn air battery was 1.5 V. Zn-air battery achieved maximum peak power density of 175 mW/cm^2 at 200 mA cm^{-2}.

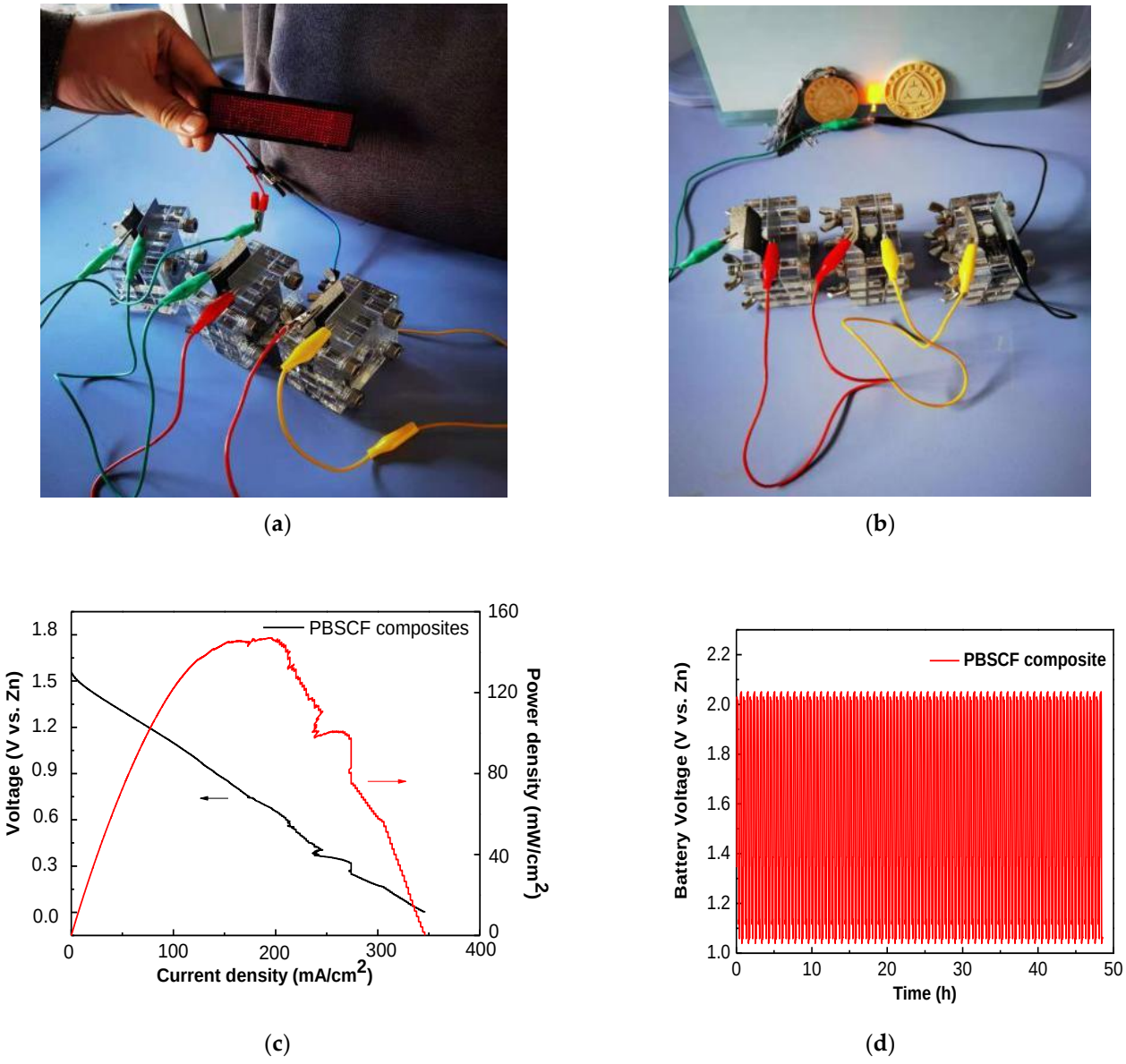

Figure 4. (**a**) OCV for three PBSCF composite Zn air batteries. (**b**) Power supplying for LED. (**c**) I–V and P–V curves for two PBSCF composite Zn-air battery cells. (**d**) Galvanostatic charge–discharge profiles of Zn-air batteries at 5 mA cm^{-2}.

The stability of the rechargeable Zn-air battery was tested by charging and discharging for 10 min individually with repeated cycles at 5 mA cm^{-2}. Its voltage gap ($\Delta\eta$) was 0.77 V initially, and the round trip efficiency was 61.9%. After 48 h, the voltage gap increased to 0.86 V and round-trip efficiency decreased to 57.6%, respectively. Such phenomenon might be due to the irreversible Zn plating-stripping process. PBSCF-composite Zn-air battery exhibits good rechargeability, and its performance is comparable to other results reported in the literature [33,34]. Moreover, PBSCF-composite is cheaper than IrO_2 and 20 Pt/C, which shows its high economic potential.

3. Experimental

3.1. Powder Preparation

$PrBa_{0.5}Sr_{0.5}Co_{1.5}Fe_{0.5}O_5$ (PBSCF) was prepared by EDTA-citrate sol-gel method. A stoichiometric amount of $Pr(NO_3)_3.H_2O$, $Ba(NO_3)_2$, $Sr(NO_3)_2$, $Co(NO_3)_3$, and $Fe(NO_3)_3.9H_2O$ (Sigma, Saint Louis, MO, USA) were weighted and mixed with distilled water, and then citric acid(CA) and EDTA (Sigma) were added. The mole ratio of n(CA):n(M^{n+}):n(EDTA)=1:1:1.5. M^{n+} indicates the total mole amount of metal ions in the mixture. After all, chemicals were mixed with water, they were heated to 80 °C for 4 h to form a dark sol. Then, it was heated to 200 °C to form a gel. In the next stage, the powders produced were combusted at 1000 °C for 5 h. PBSCF was mixed with commercial 20 wt% Pt/C from Johnson Matthey (JM). The composite obtained was denoted as PBSCF composite, in which the weight ratio of PBSCF and Pt/C was 2:1.

3.2. Electrode Preparation

Firstly, catalyst inks were prepared by mixing 10.0 mg catalyst powders, 16 μL Nafion solution and 250 μL ethanol, Secondly, they were sonicated to obtain homogeneous inks. Finally, it was dried for 5 min. Ink (5 μL) was dipped onto glassy carbon disk electrodes to achieve uniform thin film working electrodes.

3.3. Cell Preparation

2 mg PBSCF, 8 mg acetylene black, 5 mg Pt/C, 600 μL of Nafion and ethanol (1:1) were mixed together to form cell ink, and it was coated on a carbon cloth with Ni-foam. Carbon cloth and polished zinc plate were assembled in a Zn-air battery by 6 M KOH and 0.2 M $ZnCl_2$. The detailed schematic diagram used is shown in Figure 5.

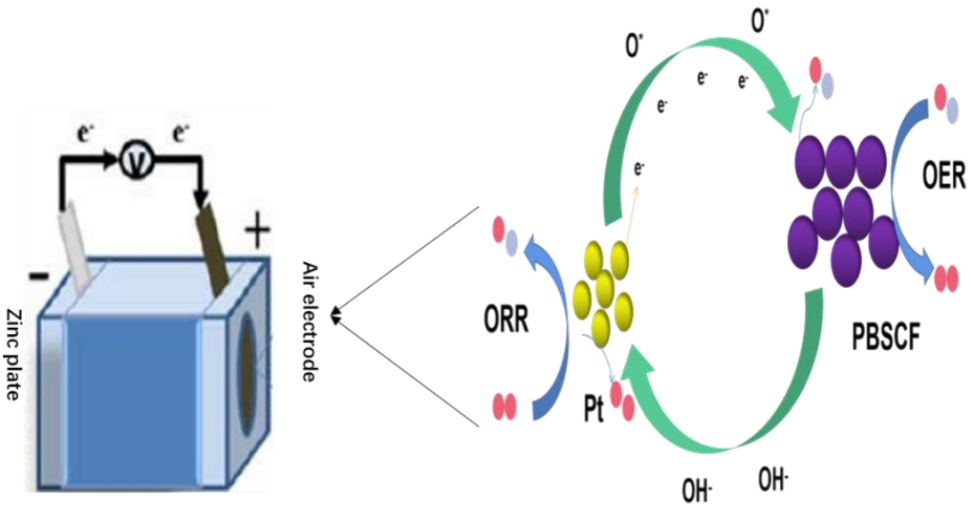

Figure 5. Schematic diagram of ORR/OER of PBSCF composite-based electrocatalysts and the assembling of rechargeable Zn-air battery.

3.4. Electrocatalyst Characterizations

XRD was used to analyse the powder phase (Bruker D8 Advances). XPS was used to test the element valence of powders by the ESCALAB 250Xi instrument (Thermo Fisher, Waltham, MA, USA). The morphology was studied by SEM (ZEISS). HRTEM images and SAED were operated at 300 kV by the JEOL-3000 instrument.

3.5. Electrocatalytic Activity Test

ORR and OER activities were measured by three-electrode method with Pt wire as a counter electrode, saturated calomel electrode as reference electrode, and glassy carbon electrode as the working electrode. Princeton electrochemical workstation with RDE system was adopted.

For the ORR test, linear sweep voltammetry (LSV) curves were tested by 10 mV/s from −1 to 0 V at different rotation speeds from 400 rpm to 2500 rpm under 0.1 M KOH. Tafel curve was also obtained under the same condition by 1 mV/s. Chronopotentiometry data was tested at a constant potential of 0.75 V (vs. RHE). For OER tests, LSV curves were tested from 0 to 1 V (vs. RHE) by 10 mV/s and at 1600 rpm. Chronoamperometry data was conducted at a constant current density of 10 mA/cm^2.

Charge and discharge data of aqueous rechargeable Zn-air battery was tested at 5 mA cm^{-2} by LAND CT2001A testing device. Polarization curves for the discharge process were tested by CHI6000A at 0.5 mA/s. The as-prepared catalyst is being used in the solid Zn-air battery in this research, and the detailed preparation process can be found in the published paper [35].

4. Conclusions

A highly active and stable ORR/OER bifunctional Pt/C-$PrBa_{0.5}Sr_{0.5}Co_{1.5}Fe_{0.5}O_5$ double perovskite electrocatalyst was used in alkaline media and its performance was monitored. $PrBa_{0.5}Sr_{0.5}Co_{1.5}Fe_{0.5}O_5$ catalyst was prepared by the sol-gel method and its composite materials showed better intrinsic ORR-OER activity and better stability in O_2-saturated 0.1 M KOH. Rechargeable Zn-air battery on PBSCF composite demonstrated good initial discharge and charge potential. In addition, it also exhibited high cycling stability after 48 h. Overall, all these results illustrate that PBSCF composite is an economical electrocatalyst for rechargeable Zn-air batteries.

Author Contributions: Conceptualization, C.W.; methodology, Z.Z.; software, Z.C.; validation, X.L.; formal analysis, B.H.; investigation, M.G.; resources, X.G.; data curation, X.F.; writing—original draft preparation, Z.T.; funding acquisition, C.W. All authors have read and agreed to the published version of the manuscript.

Funding: This research was funded by 2022 Shenzhen Science and Technology Program (GJHZ20210705142006020), 2022 Research Funding of Shenzhen Polytechnic (6022310007K), Sichuan science and technology program (2020YJ0501,2022YFH0044).

Acknowledgments: The authors acknowledge the facilities, the scientific and technical assistance from Hoffman Research Institute in Shenzhen Polytechnic.

Conflicts of Interest: The authors declare no conflict of interest.

References

1. Cao, R.; Lee, J.S.; Liu, M.L.; Cho, J. Recent Progress in Non-Precious Catalysts for Metal-Air Batteries. *Adv. Energy Mater.* **2012**, *2*, 816–829. [CrossRef]
2. Li, H.; Ma, L.; Han, C.; Wang, Z.; Liu, Z.; Tang, Z.; Zhi, C. Advanced rechargeable zinc-based batteries: Recent progress and future perspectives. *Nano Energy* **2019**, *62*, 550–587. [CrossRef]
3. Pan, J.; Xu, Y.Y.; Yang, H.; Dong, Z.; Liu, H.; Xia, B.Y. Advanced Architectures and Relatives of Air Electrodes in Zn-Air Batteries. *Adv. Sci.* **2018**, *5*, 1700691. [CrossRef] [PubMed]
4. Park, J.; Park, M.; Nam, G.; Lee, J.S.; Cho, J. All-Solid-State Cable-Type Flexible Zinc-Air Battery. *Adv. Mater.* **2015**, *27*, 1396. [CrossRef] [PubMed]
5. Nie, Y.; Li, L.; Wei, Z. Recent advancements in Pt and Pt-free catalysts for oxygen reduction reaction. *Chem. Soc. Rev.* **2015**, *44*, 2168–2201. [CrossRef]
6. Shi, Q.; Zhu, C.; Du, D.; Lin, Y. Robust noble metal-based electrocatalysts for oxygen evolution reaction. *Chem. Soc. Rev.* **2019**, *48*, 3181–3192. [CrossRef]
7. Wang, Q.; Shang, L.; Shi, R.; Zhang, X.; Zhao, Y.F.; Waterhouse, G.I.N.; Wu, L.Z.; Tung, C.H.; Zhang, T.R. NiFe Layered Double Hydroxide Nanoparticles on Co, N-Co doped Carbon Nanoframes as Efficient Bifunctional Catalysts for Rechargeable Zinc-Air Batteries. *Adv. Energy Mater.* **2017**, *7*, 21.
8. Meng, F.L.; Liu, K.H.; Zhang, Y.; Shi, M.M.; Zhang, X.B.; Yan, J.M.; Jiang, Q. Recent Advances toward the Rational Design of Efficient Bifunctional Air Electrodes for Rechargeable Zn-Air Batteries. *Small* **2018**, *14*, 1703843. [CrossRef]
9. Lopez, K.; Park, G.; Sun, H.J.; An, J.C.; Eom, S.; Shim, J. Electrochemical characterizations of $LaMO_3$ (M=Co, Mn, Fe, and Ni) and partially substituted $LaNi_xM_{1-x}O_3$ (x=0.25 or 0.5) for oxygen reduction and evolution in alkaline solution. *J. Appl. Electrochem.* **2015**, *45*, 313–323. [CrossRef]

10. Bu, Y.; Gwon, O.; Nam, G.; Jang, H.; Kim, S.; Zhong, Q.; Kim, G. A highly effcient and robust cation ordered perovskite oxide as a bifunctional catalyst for re-chargeable zinc-air batteries. *ACS Nano* **2017**, *11*, 11594–11601. [CrossRef]
11. Lee, D.U.; Park, H.W.; Park, M.G.; Ismayilov, V.; Chen, Z. Synergistic bifunctional catalyst design based on perovskite oxide nanoparticles and intertwined carbon nanotubes for rechargeable zinc-air battery applications. *ACS Appl. Mater. Interfaces* **2014**, *7*, 902–910. [CrossRef] [PubMed]
12. Chen, D.; Wang, J.; Zhang, Z.; Shao, Z.; Ciucci, F. Boosting oxygen reduction/evolution reaction activities with layered perovskite cata-lysts. *Chem. Commun.* **2016**, *52*, 10739–10742. [CrossRef] [PubMed]
13. Jin, C.; Cao, X.C.; Zhang, L.Y.; Zhang, C.; Yang, R. Preparation and electrochemical properties of urchin-like $La_{0.8}Sr_{0.2}MnO_3$ perovskite oxide as a bifunctional catalyst for oxygen reduction and oxygen evolution reaction. *J. Power Sources* **2013**, *241*, 225–230. [CrossRef]
14. Suntivich, J.; May, K.J.; Gasteiger, H.A.; Goodenough, J.B.; Shao-Horn, Y. A Perovskite Oxide Optimized for Oxygen Evolution Catalysis from Molecular Orbital Principles. *Science* **2011**, *334*, 1383–1385. [CrossRef]
15. Suntivich, J.; Gasteiger, H.A.; Yabuuchi, N.; Nakanishi, H.; Goodenough, J.B.; Shao-Horn, Y. Design principles for oxy-gen-reduction activity on perovskite oxide catalysts for fuel cells and metal-air batteries. *Nat. Chem.* **2011**, *3*, 546–550. [CrossRef] [PubMed]
16. Zhu, Y.; Zhou, W.; Yu, J.; Chen, Y.; Liu, M.; Shao, Z. Enhancing Electrocatalytic Activity of Perovskite Oxides by Tuning Cation Deficiency for Oxygen Reduction and Evolution Reactions. *Chem. Mater.* **2016**, *28*, 1691–1697. [CrossRef]
17. Lee, J.G.; Hwang, J.; Hwang, H.J.; Jeon, O.S.; Jang, J.; Kwon, O.; Lee, Y.; Han, B.; Shul, Y.-G. A New Family of Perovskite Catalysts for Oxygen-Evolution Reaction in Alkaline Media: $BaNiO_3$ and $BaNi_{0.83}O_2$. *J. Am. Chem. Soc.* **2016**, *138*, 3541–3547. [CrossRef]
18. Zhu, Y.; Zhou, W.; Sunarso, J.; Zhong, Y.; Shao, Z. Phosphorus-Doped Perovskite Oxide as Highly Efficient Water Oxidation Elec-trocatalyst in Alkaline Solution. *Adv. Funct. Mater.* **2016**, *26*, 5862–5872. [CrossRef]
19. Zhou, W.; Sunarso, J. Enhancing Bi-functional Electrocatalytic Activity of Perovskite by Temperature Shock: A Case Study of $LaNiO_{3-d}$. *J. Phys. Chem. Lett.* **2013**, *4*, 2982–2988. [CrossRef]
20. Zhang, D.; Song, Y.; Du, Z.; Wang, L.; Li, Y.; Goodenough, J.B. Active $LaNi_{1-x}Fe_xO_3$ bifunctional catalysts for air cathodes in alkaline media. *J. Mater. Chem. A* **2015**, *3*, 9421–9426. [CrossRef]
21. Su, C.; Wang, W.; Chen, Y.; Yang, G.; Xu, X.; Tade, M.O.; Shao, Z. $SrCo_{0.9}Ti_{0.1}O_{3-d}$ As a New Electrocatalyst for the Oxy-gen Evolu-tion Reaction in Alkaline Electrolyte with Stable Performance. *ACS Appl. Mater. Interfaces* **2015**, *7*, 17663–17670. [CrossRef] [PubMed]
22. Xu, X.; Pan, Y.; Zhou, W.; Chen, Y.; Zhang, Z.; Shao, Z. Toward Enhanced Oxygen Evolution on Perovskite Oxides Synthesized from Different Approaches: A Case Study of $Ba_{0.5}Sr_{0.5}Co_{0.8}Fe_{0.2}O_{3-d}$. *Electrochim. Acta* **2016**, *219*, 553–559. [CrossRef]
23. Jung, J.-I.; Jeong, H.Y.; Lee, J.-S.; Kim, M.G.; Cho, J. A Bifunctional Perovskite Catalyst for Oxygen Reduction and Evolution. *Angew. Chem. Int. Ed.* **2014**, *53*, 4582–4586. [CrossRef] [PubMed]
24. Wang, C.C.; Cheng, Y.; Ianni, E.; Lin, B. A highly active and stable $La_{0.5}Sr_{0.5}Ni_{0.4}Fe_{0.6}O_{3-\delta}$ perovskite electrocatalyst for oxygen evolution reaction in alkaline media. *Electrochim. Acta* **2018**, *246*, 997–1003. [CrossRef]
25. Wang, X.; Sunarso, J.; Lu, Q.; Zhou, Z.; Dai, J.; Guan, D.; Zhou, W.; Shao, Z. High-Performance Platinum-Perovskite Composite Bifunctional Oxygen Electrocatalyst for Rechargeable Zn-Air Battery. *Adv. Energy Mater.* **2019**, *10*, 1903271. [CrossRef]
26. Zhu, Y.; He, Z.; Choi, Y.; Chen, H.; Li, X.; Zhao, B.; Yu, Y.; Zhang, H.; Stoerzinger, K.A.; Feng, Z.; et al. Tuning proton-coupled electron transfer by crystal orientation for efficient water oxidization on double perovskite oxides. *Nat. Commun.* **2020**, *11*, 4299. [CrossRef] [PubMed]
27. Sun, H.N.; Chen, G.; Sunarso, J.; Dai, J.; Zhou, W.; Shao, Z.P. Molybdenum and Niobium Codoped B-Site-Ordered Double Per-ovskite Catalyst for Efficient Oxygen Evolution Reaction. *ACS Appl. Mater. Interfaces* **2018**, *20*, 16939–16942. [CrossRef]
28. Tang, K.; Yuan, C.Z.; Xiong, Y.; Hu, H.B.; Wu, M.Z. Inverse-opal-structured hybrids of N, S-co doped-carbon-confined Co_9S_8 nanoparticles as bifunctional oxygen electrocatalyst for on-chip all-solid-state rechargeable Zn-air batteries. *Appl. Catal. B Environ.* **2020**, *260*, 118209. [CrossRef]
29. Kumar, R.; Shin, J.; Yin, L.; You, J.M.; Meng, Y.S.; Wang, J. All-Printed, Stretchable Zn-Ag_2O Rechargeable Battery via Hyperelastic Binder for Self-Powering Wearable Electronics. *Adv. Energy Mater.* **2017**, *7*, 1602096. [CrossRef]
30. Li, H.; Han, C.; Huang, Y.; Huang, Y.; Zhu, M.; Pei, Z.; Xue, Q.; Wang, Z.; Liu, Z.; Tang, Z.; et al. An extremely safe and wearable solid-state zinc ion battery based on a hierarchical structured polymer electrolyte, Energy Envi-ronmental. *Science* **2018**, *11*, 941–951.
31. Liu, X.; Wang, L.; Yu, P.; Tian, C.; Sun, F.; Ma, J.; Li, W.; Fu, H. A Stable Bifunctional Catalyst for Rechargeable Zinc-Air Batteries: Iron-Cobalt Nanoparticles Embedded in a Nitrogen-Doped 3D Carbon Matrix. *Angew. Chem. Int. Ed.* **2018**, *57*, 16166–16170. [CrossRef] [PubMed]
32. Su, C.Y.; Cheng, H.; Li, W.; Liu, Z.Q.; Li, N.; Hou, Z.; Bai, F.Q.; Zhang, H.X.; Ma, T.Y. Atomic modulation of FeCo–nitrogen–carbon bifunctional oxygen electrodes for rechargeable and flexible all-solid-state zinc–air battery. *Adv. Energy Mater.* **2017**, *7*, 1602420. [CrossRef]
33. Yang, F.; Liu, X.; Zhang, H.; Zhou, J.; Jiang, J.; Lu, X. Boosting oxygen catalytic kinetics of carbon nanotubes by oxygen-induced electron density modulation for advanced Zn-air batteries. *Energy Storage Mater.* **2020**, *30*, 138–145. [CrossRef]

34. Zhu, L.; Zheng, D.; Wang, Z.; Zheng, X.; Fang, P.; Zhu, J.; Lu, X. A Confinement Strategy for Stabilizing ZIF-Derived Bifunctional Catalysts as a Benchmark Cathode of Flexible All-Solid-State Zinc-Air Batteries. *Adv. Mater.* **2018**, *30*, 1805268. [CrossRef] [PubMed]
35. Wang, W.; Tang, M.; Zheng, Z.; Chen, S. Alkaline Polymer Membrane-Based Ultrathin, Flexible, and High-Performance Solid-State Zn air battery. *Adv. Energy Mater.* **2019**, *9*, 1901718. [CrossRef]